Journal of Pharmaceutical and Biomedical Analysis 78–79 (2013) 1–8

Contents lists available at SciVerse ScienceDirect

Journal of Pharmaceutical and Biomedical Analysis

journal homepage: www.elsevier.com/locate/jpba

Redox-proteomic analysis of doxorubicin resistance-induced altered thiol activity in uterine carcinoma

Szu-Ting Lin[a,1], Yi-Wen Lo[b,1], Shing-Jyh Chang[c,d], Wen-Ching Wang[e], Margaret Dah-Tsyr Chang[e], Ping-Chiang Lyu[a], Yi-Wen Chen[a], Hsiu-Chuan Chou[b,**], Hong-Lin Chan[a,*]

[a] Department of Medical Science and Institute of Bioinformatics and Structural Biology, National Tsing Hua University, Hsinchu, Taiwan
[b] Department of Applied Science, National Hsinchu University of Education, Hsinchu, Taiwan
[c] Department of Obstetrics and Gynecology, MacKay Memorial Hospital Hsinchu Branch, Hsinchu, Taiwan
[d] Department of Nursing, Yuanpei University, Hsinchu, Taiwan
[e] Department of Medical Science and Institute of Molecular and Cellular Biology, National Tsing Hua University, Hsinchu, Taiwan

ARTICLE INFO

Article history:
Received 30 November 2012
Received in revised form 16 January 2013
Accepted 19 January 2013
Available online xxx

Keywords:
Redox-proteomics
DIGE
Doxorubicin
Resistance
MALDI-TOF MS

ABSTRACT

Doxorubicin is an anticancer drug used in a wide range of cancer therapies; however, doxorubicin-induced drug resistance is one of the most serious obstacles of cancer chemotherapy. Recent studies have indicated that reduced oxidative stress levels in cancer cells induce drug resistance. However, the redox-modifications of resistance – associated cellular targets are largely unknown. Thus, the current study employed cysteine-labeling based two-dimensional differential gel electrophoresis (2D-DIGE) combined with MALDI-TOF mass spectrometry (MALDI-TOF MS) to analyze the effect of doxorubicin resistance on redox regulation in uterine cancer and showed 33 spots that were significantly changed in thiol reactivity. These proteins involve cytoskeleton regulation, signal transduction, redox-regulation, glycolysis, and cell-cycle regulation. The current work shows that the redox 2D-DIGE-based proteomic strategy provides a rapid method to study the molecular mechanisms of doxorubicin-induced drug resistance in uterine cancer. The identified targets may be used to further evaluate their roles in drug-resistance formation and for possible diagnostic or therapeutic applications.

1. Introduction

Drug resistance is one of the main obstacles during the process of cancer chemotherapy. The exact mechanism of drug resistance is complex and poor understood. The most potential factors for resistance include over-expression of ABC transporter, reduced drug uptake, enhanced drug detoxification, decreased apoptosis and increased DNA repair system [1]. Doxorubicin is one of the anti-cancer drug has been used clinically for decades to treat a number of cancers, such as breast cancer, lung cancer and many other carcinoma types [2–5]. However, some of the side effects of doxorubicin treatment have been reported and one of these is the doxorubicin-induced drug resistance.

Reactive oxygen species (ROS) are species of oxygen which are in a more reactive state than molecular oxygen, and in which the oxygen is reduced to varying degrees. ROS comprise several species such as hydrogen peroxide, the hydroxyl radical, superoxide and singlet oxygen. $O2^{-}$ can be generated by the action of such enzymes as NADPH oxidase, lipoxygenase, cyclooxygenase, cytochrome P450 or through UV irradiation and can be converted into H_2O_2 and O_2 by the action of superoxide dismutases. H_2O_2 can be also further converted to $^{\cdot}OH$ in the presence of Fe^{2+} [6,7]. In general, high concentrations of ROS have been observed in most cancers, in which these ROS promote cancer progression and development. Numerous anticancer drugs including doxorubicin work by further increasing cellular concentrations of ROS to overcome the detoxification and anti-oxidant ability of the cancer cells [8]. Recent studies indicated that adaptation of the concentrations of intracellular anti-oxidants could result in drug resistance. For example, reduced glutathione levels are increased in numerous cancers that show elevated resistance against chemotherapeutic drugs [9,10]. These processes are mediated by intracellular redox-regulation enzymes such as alpha-glutamycysteine synthetase [11], catalase [12] and glutathione reductase [13].

Abbreviations: 2D-DIGE, two-dimensional differential gel electrophoresis; CCB, colloidal coomassie blue; ICy dyes, iodoacetyl cyanine dyes; MALDI-TOF MS, matrix assisted laser desorption ionization-time of flight mass spectrometry; mPR, membrane-associated progesterone receptor component 1; ROS, reactive oxygen species.

* Corresponding author at: Institute of Bioinformatics and Structural Biology & Department of Medical Sciences, National Tsing Hua University, No. 101, Kuang-Fu Rd. Sec. 2, Hsinchu 30013, Taiwan. Tel.: +886 3 5742476; fax: +886 3 5715934.
** Corresponding author. Tel.: +886 3 5213132x2721; fax: +886 3 5257178.
E-mail addresses: chouhc@mail.nhcue.edu.tw (H.-C. Chou), hlchan@life.nthu.edu.tw (H.-L. Chan).
[1] These authors contributed equally to this work.

0731-7085/$ – see front matter © 2013 Elsevier B.V. All rights reserved.
http://dx.doi.org/10.1016/j.jpba.2013.01.028

Proteomics is a powerful tool to monitor protein expression and post-translational modification of proteins in response to specific treatment. 2-DE remains an important technique in proteomics for global protein profiling within biological samples and plays a complementary role to LC–MS-based analysis. However, reliable quantitative comparison between gels remains the primary challenge in 2-DE analysis. A significant improvement in gel-based protein detection and quantification was achieved by the introduction of 2D-DIGE, where several samples can be co-detected on the same gel using differential fluorescent labeling. This approach alleviates gel-to-gel variation and allows comparison of the relative amount of resolved proteins across different gels using a fluorescently-labeled internal standard. Moreover, the 2D-DIGE technique has the advantages of a broader dynamic range of detection, higher sensitivity and greater reproducibility than traditional 2-DE [14]. Recently, a cysteine labeling version of 2D-DIGE was developed, using ICy dyes (iodoacetyl cyanine dyes) which react with the free thiol group of cysteines *via* alkylation. The paired of ICy dyes (ICy3 and ICy5) have been used to monitor redox-dependent protein thiol modifications in model cell systems [15,16].

In our previous publication, 37 proteins have been reported to show differentially expressed between uterine cancer cell and its derived resistant line. In which, asparagine synthetase and membrane-associated progesterone receptor component 1 (mPR) are both evidenced to be essential for the formation of doxorubicin-induced drug resistance [5]. Followed study demonstrated that decreased oxidative stress levels were observed in doxorubicin resistance cancer cells; however, the redox-modifications of resistance-associated cellular targets have not been reported in our knowledge. Accordingly, the aim of this investigation was to conduct an *in vitro* investigation into doxorubicin-induced drug resistance using quantitative redox-proteomic strategies including ICy dyes-based labeling and MALDI-TOF MS to monitor redox-dependent protein thiol modifications, to increase the understanding of the molecular processes involved, and to identify potential drug resistance biomarkers with possible diagnostic or therapeutic applications.

2. Materials and methods

2.1. Chemicals and reagents

Generic chemicals were purchased from Sigma–Aldrich (St. Louis, MO, USA), while reagents for 2D-DIGE were purchased from GE Healthcare (Uppsala, Sweden). The synthesis of the ICy3 and ICy5 dyes has been previously reported in previous publication [17]. All primary antibodies were purchased from Genetex (Hsinchu, Taiwan) and anti-mouse, and anti-rabbit secondary antibodies were purchased from GE Healthcare. All the chemicals and biochemicals used in this study were of analytical grade.

2.2. Cell lines and cell culture

The uterine sarcoma cancer line MES-SA was purchased from American Type Culture Collection, (Manassas, VA, USA). The doxorubicin resistance line MES-SA/DxR cell was cultured in McCoy's 5a modified medium containing 10% fetal bovine serum, L-glutamine (2 mM), streptomycin (100 μg/mL), penicillin (100 IU/mL) (all from Gibco-Invitrogen Corp., Paisley, UK) and maintained with 0.6 μM doxorubicin. All cells were incubated at 37 °C in a humidified atmosphere containing 5% CO_2. Cells were passaged at 80–90% confluence by trypsinization according to standard procedures.

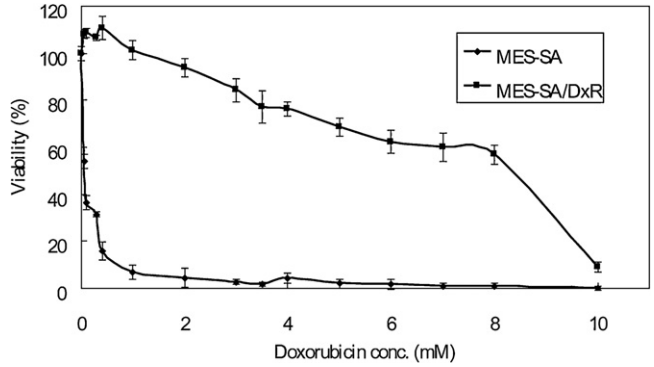

Fig. 1. Dose-dependent kinetics of doxorubicin-induced loss of cell viability in MES-SA and MES-SA/DxR cells. MES-SA and MES-SA/DxR cells grown overnight were treated with a range of doses of doxorubicin and cell viability was determined by MTT assay.

2.3. Assay for endogenous reactive oxygen species using DCFH-DA

MES-SA and MES-SA/DxR cells (10,000 cells/well) were incubated with the indicated concentrations of doxorubicin for 20 min. After two washes with PBS, cells were treated with 10 μM of 2,7-dichlorofluorescin diacetate (DCFH-DA; Molecular Probes) at 37 °C for 20 min, and subsequently washed with PBS. Fluorescence was recorded at an excitation wavelength 485 nm and emission wavelength at 530 nm with Gemini fluorescence microplate reader (Molecular Devices, Sunnyvale, CA, USA).

2.4. MTT cell viability assay

MES-SA and MES-SA/DxR cells growing exponentially were trypsinized, counted using a haemocytometer and 10,000 cells/well were seeded into 96-well plates. The culture was then incubated for 24 h before pre-treatment with the indicated concentrations of doxorubicin for 20 min or left untreated. After removal of the medium, 50 μL of MTT working solution (1 mg/mL) was added to the cells in each well, followed by a further incubation at 37 °C for 4 h. The supernatant was carefully removed. 100 μL of DMSO was added to each well and the plates shaken for 20 min. The absorbance of samples was then measured at 540 nm in a multi-well plate reader. Values were normalized against the untreated samples and were averaged from 4 independent measurements.

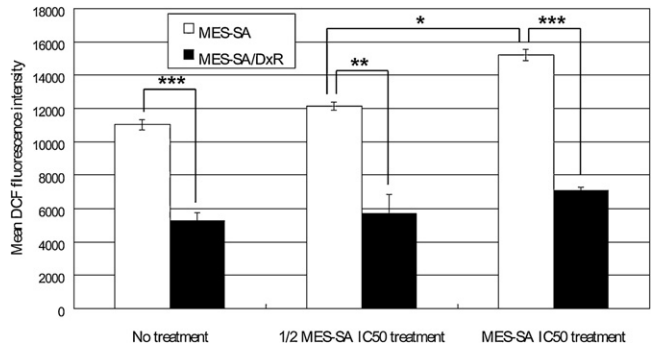

Fig. 2. Effect of doxorubicin-resistance on MES-SA and MES-SA/DxR ROS levels. 100,000 MES-SA and MES-SA/DxR cells were used for DCFH-based intracellular ROS production assays. The cells were treated with the indicated concentrations of doxorubicin for 20 min followed by treated with 10 μM of DCFH-DA at 37 °C for 20 min and the levels of cellular ROS were determined with fluorescence reader to record at excitation and emission wavelengths of 485 nm and 530 nm, respectively. All of statistic comparisons used in this study were performed with paired Student's *t*-test. $^{*}p < 0.05$, $^{**}p < 0.01$ and $^{***}p < 0.001$ indicate significant differences between the experiments.

Table 1
Differential cysteine labeled proteins identified by ICy 2D-DIGE and MALDI-TOF MS.

Spot No.	Swiss-prot No.	Gene name	Protein name	MW	Theoretical pI	Observed pI	No. Match. Peptides	Cov. (%)	MOWSE Score	Subcellular location	Functional ontology	Matched peptide[a]	MES-SA/DxR/MES-SA (cys/lys)[b]
1788	Q99714	HSD17B10	3-Hydroxyacyl-CoA dehydrogenase type-2	27,134	7.66	7.90	7/18	29%	74/56	Mitochondrion	tRNA processing	VCNFLASQVPFPSR/DLAPIGIR	1.79
1600	O95336	PGLS	6-Phosphogluconolactonase/6PGL	27,815	5.70	6.80	4/15	20%	63/56	Cytoplasm	Pentose phosphate pathway	ELPAAVAPAGPASLAR	1.81
717	P00352	ALDH1A1	Aldehyde dehydrogenase family 1 member A1/RALDH1	55,454	6.30	7.60	11/23	23%	81/56	Cytoplasm	Redox regulation	QAFQIGSPWR	−1.94
748	P00352	ALDH1A1	Aldehyde dehydrogenase family 1 member A1/RALDH1	55,454	6.30	7.50	8/18	17%	71/56	Cytoplasm	Redox regulation	EEIFGPVQQIMK/IFVEESIYDEFVR	−1.66
818	P06733	ENO1	Alpha-enolase/MBP1	47,481	7.01	7.90	8/23	20%	89/56	Plasma membrane	Glycolysis	AAVPSGASTGIYEALELR	1.89
785	Q86XL3	ANKLE2	Ankyrin repeat and LEM domain-containing protein 2/KIAA0692	104,912	6.56	8.50	10/26	10%	56/56	Plasma membrane	Protein–Protein interaction	EEIVKAGLK	1.52
804	Q86XL3	ANKLE2	Ankyrin repeat and LEM domain-containing protein 2/KIAA0692	104,912	6.56	8.00	10/31	11%	57/56	Plasma membrane	Protein–Protein interaction	KLAQALLEQGGR	1.72
706	Q8NEU8	APPL2	DCC-interacting protein 13-beta/Dip13-beta	74,959	4.87	5.00	7/26	14%	56/56	Nucleus	Cell cycle	VYGAQNEMCLATQQLSK	1.48
1734	Q8NEU8	APPL2	DCC-interacting protein 13-beta/Dip13-beta	74,959	4.87	5.10	6/17	12%	64/56	Nucleus	Cell cycle	VYGAQNEMCLATQQLSK	1.67
1527	Q8NEU8	APPL2	DCC-interacting protein 13-beta/Dip13-beta	74,959	4.87	5.60	6/17	12%	57/56	Nucleus	Cell cycle	VYGAQNEMCLATQQLSK	2.05
2107	P09382	LGALS1	Galectin-1/Gal-1	15,048	5.34	5.50	6/50	51%	73/56	Secreted	Cell migration	VRGEVAPDAK/DGGAWGTEQR	−1.66
1814	Q9UC36	HSPB1	Heat shock protein beta-1/HspB1/HSP27	22,826	5.98	6.20	6/29	27%	67/56	Cytoplasm	Protein folding	VPFSLLR/GPSWDPFR	−1.79
670	P31943	HNRNPH1	Heterogeneous nuclear ribonucleoprotein H/hnRNP H	49,484	5.89	6.40	5/14	15%	70/56	Nucleus	RNA processing	VHIEIGPDGR/GLPWSCSADEVQR	1.44
1882	P04264	KRT1	Keratin, type II cytoskeletal 1/CK-1	66,149	8.15	5.60	5/14	12%	58/56	Cytoplasm	Cytoskeleton	SLNNQFASFIDK	−1.49
1910	P04264	KRT1	Keratin, type II cytoskeletal 1/CK-1	66,149	8.15	6.60	8/22	12%	69/56	Cytoplasm	Cytoskeleton	NMQDMVEDYR/SLNNQFASFIDK	3.86
1511	P04264	KRT1	Keratin, type II cytoskeletal 1/CK-1	66149	8.15	5.50	9/47	20%	85/56	Cytoplasm	Cytoskeleton	SLDLDSIIAEVK/TNAENEFVTIK	1.50
1160	A6NJI9	LRRC72	Leucine-rich repeat-containing protein 72	33,863	8.91	7.50	7/31	25%	58/56	Nucleus	Unknown	SWDPNPVPRTLR	1.64
642	Q6UXM1	LRIG3	Leucine-rich repeats and immunoglobulin-like domains protein 3/LIG-3	125,066	5.79	7.00	6/21	7%	67/56	Plasma membrane	Signal transduction	TPNFQSYDLDT/VTSMEPGYFDNLANTLLVLK	1.75
1138	Q14168	MPP2	MAGUK p55 subfamily member 2/Discs large homolog 2/DLG2/MPP2	64,887	6.28	7.00	8/33	15%	57/56	Plasma membrane	Signal transduction	YFGAHERLEETK	1.40
1854	O00264	PGRMC1	Membrane-associated progesterone receptor component 1	21,772	4.56	5.20	7/24	30%	95/56	Microsome	Signal transduction	DFTPAELR/RFDGVQDPR	−2.08
1509	Q9UI09	NDUFA12	NADH dehydrogenase [ubiquinone] 1 alpha subcomplex subunit 12/DAP13	17,104	9.63	6.00	5/22	33%	58/56	Mitochondrion	Electron transport	MELVQVLKR	1.44
1857	Q06830	PRDX1	Peroxiredoxin-1	22,324	8.27	8.50	7/24	29%	75/56	Cytoplasm	Redox regulation	QITVNDLPVGR/QITVNDLPVGR	−5.15
1933	P32119	PRDX2	Peroxiredoxin-2	22,049	5.66	6.70	8/18	28%	96/56	Cytoplasm	Redox regulation	IGKPAPDFK/RLSEDYGVLK	−1.53
691	P01148	GNRH1	Progonadoliberin-1/Gonadotropin-releasing hormone I/GnRH-I	10,544	6.10	6.60	5/20	44%	68/56	Secreted	Hormone secretion	EVGQLAETQR	1.63

Table 1 (*Continued*)

Spot No.	Swiss-prot No.	Gene name	Protein name	MW	Theoretical pI	Observed pI	No. Match. Peptides	Cov. (%)	MOWSE Score	Subcellular location	Functional ontology	Matched peptide[a]	MES-SA/DxR/MES-SA (cys/lys)[b]
2053	Q8N1K5	THEMIS	Protein THEMIS/C6orf190/Thymocyte-expressed molecule involved in selection	74,033	5.62	5.20	6/18	9%	56/56	Nucleus	Immune response	LENLIIK	3.40
482	P14618	PKM2	Pyruvate kinase isozymes M1/M2/PKM	58,470	7.96	8.10	5/9	15%	72/56	Cytoplasm	Glycolysis	NTGIICTIGPASR	1.38
1339	Q969Q6	PPP2R3C	Serine/threonine-protein phosphatase 2A regulatory subunit B" subunit gamma	53,567	5.07	7.60	7/27	18%	57/56	Cytoplasm	Signal transduction	EPAALQYIFK/AIQELMKIHGQDPVSFQDVK	−1.55
2058	O00743	PPP6C	Serine/threonine-protein phosphatase 6 catalytic subunit/PP6C	35,806	5.43	5.30	4/13	10%	57/56	Cytoplasm	Signal transduction	MAPLDLDK	1.76
1723	P60174	TPI1	Triosephosphate isomerase/TIM/TPI	31,057	5.65	7.80	12/23	55%	148/56	Cytoplasm	Glycolysis	FFVGGNWK/IAVAAQNCYK	1.38
1719	P60174	TPI1	Triosephosphate isomerase/TIM/TPI	31,057	5.65	7.20	6/31	29%	78/56	Cytoplasm	Glycolysis	VPADTEVVCAPPTAYIDFAR/FFVGGNWK	1.40
680	Q8N850	VIM	Vimentin	53,676	5.06	6.50	12/61	25%	125/56	Cytoplasm	Cytoskeleton	SVSSSSYR/FLEQQNK	1.70
669	Q8N850	VIM	Vimentin	53,676	5.06	6.30	8/54	19%	67/56	Cytoplasm	Cytoskeleton	FADLSEAANR/DNLAEDIMR	1.53
667	Q8N850	VIM	Vimentin	53,676	5.06	6.20	6/25	14%	66/56	Cytoplasm	Cytoskeleton	FADLSEAANR/EEAENTLQSFR	1.41

Proteins displaying doxorubicin resistance-induced differential labeling of cysteines and lysines using ICy dyes and NHS-Cy2 dyes, respectively, were identified by MALDI-TOF peptide mass mapping analysis. Proteins displaying an average fold-difference of ≥1.3-fold where $p < 0.05$ and spots matched in all images are listed in this table.

[a] In MS analysis, the table listed top score peptide sequence in the matched peptide column.

[b] To accurately calculate doxorubicin-induced differential labeling of cysteines in consideration of protein level alterations, the cysteine-labeling ratios were normalized using the lysine-labeling ratios.

Fig. 3. Redox 2D-DIGE analysis of doxorubicin-induced differential cysteine-modification in MES-SA and MES-SA/DxR cells. Lysates from MES-SA and MES-SA/DxR cells were subjected to redox-2D-DIGE analysis as described in Section 2. (A) Protein sample arrangement for a triplicate redox 2D-DIGE experiment. (B) Differentially labeled protein features are annotated with spot numbers.

2.5. Redox-2D-DIGE and gel image analysis

For redox DIGE analysis, MES-SA and MES-SA/DxR cells were treated with 0.05 μM (0.5 × IC50 of doxorubicin on MES-SA), 0.1 μM (1 × IC50 of doxorubicin on MES-SA) of doxorubicin for 20 min or left untreated. These treated cells were lysed in 2-DE buffer (CHAPS (4% w/v), urea (8 M), Tris–HCl (pH 8.3; 10 mM) and EDTA (1 mM)) in the presence of ICy3 or ICy5 (80 pmol/mg protein) on ice to limit post-lysis thiol modification. Protein samples (100 μg) coming from MES-SA and MES-SA/DxR cells were labeled with the ICy5 dye, respectively, and mixed with an equal amount of a standard pool of protein samples (100 μg) coming from MES-SA and MES-SA/DxR cells labeled with ICy3. Since ICy dyes interfered with the protein assay, protein concentrations were determined on replica lysates not containing dye. Lysates were left in the dark for 1 h followed by labeling with Cy2 to monitor protein level. The reactions were quenched with DTT (65 mM final concentration) for 10 min followed by L-lysine (20-fold molar ratio excess of free L-lysine to Cy2 dye) for a further 10 min. Volumes were adjusted to 450 μL with buffer plus DTT and IPG buffer for rehydration. Isoelectric focusing was then performed using a Multiphor II apparatus (GE Healthcare) for a total of 62.5 kVh at 20 °C. Strips were then equilibrated in urea (6 M), glycerol (30%, v/v), SDS (1%, w/v), Tris–HCl

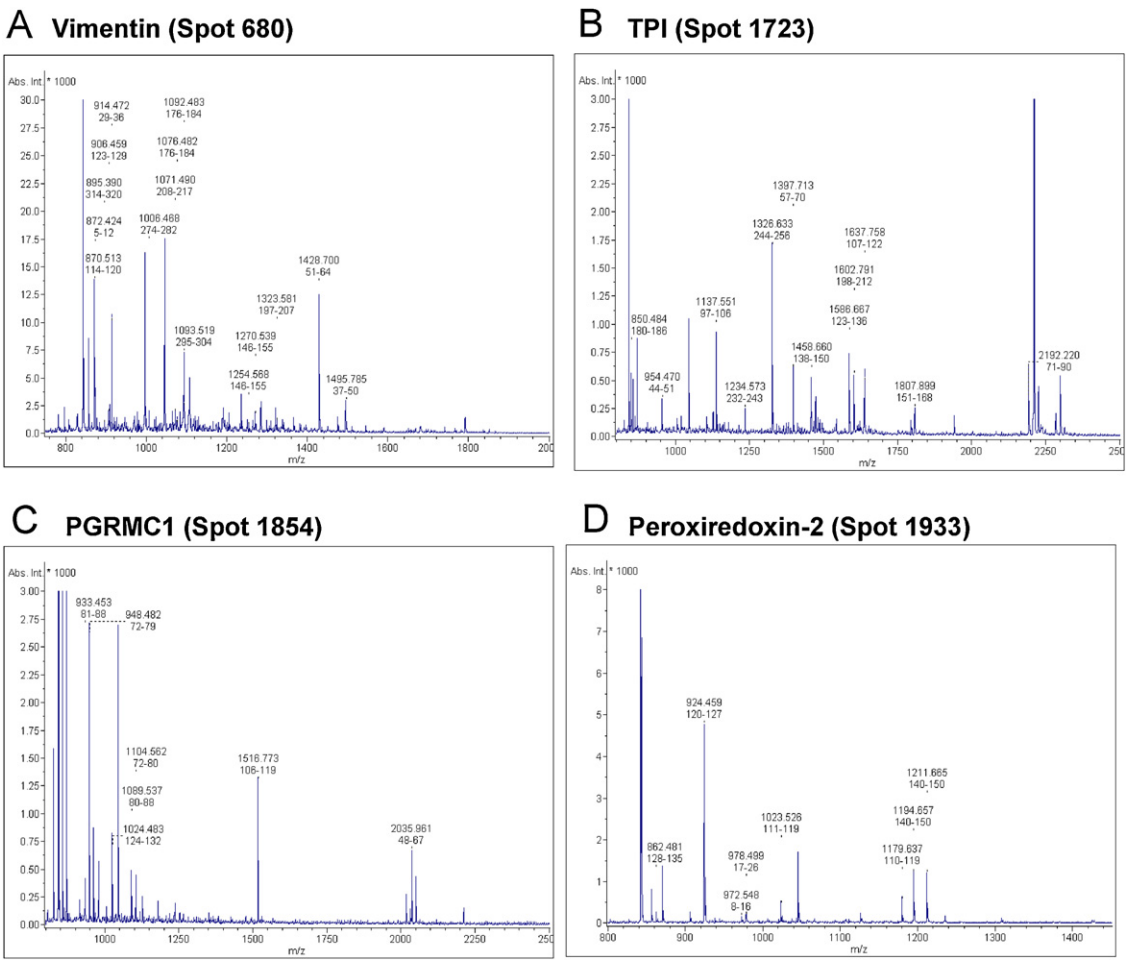

Fig. 4. Peptide mass fingerprinting of differentially labeling proteins ((A) vimentin (B) TPI (C) PGRMC1 (D) peroxiredoxin 2). Mass spectra were acquired on an Autoflex TOF/TOF mass spectrometer. Peptides contribute to protein identifications were marked with *m*/*z* values and sequence locations on proteins which were searched against the Swiss-Prot/TrEMBL database using Mascot software.

(pH 8.8; 100 mM) with dithiothreitol (65 mM) for 15 min and then in the same buffer containing iodoacetamide (240 mM) for a further 15 min. Equilibrated IPG strips were transferred onto 24 cm × 20 cm 12.5% polyacrylamide gels cast between low-fluorescence glass plates and bonded to one of the plates. The strips were overlaid with low melting point agarose (0.5%, w/v) in running buffer containing bromophenol blue. The gels were run in an Ettan Twelve gel tank (GE Healthcare) at 4 W per gel at 10 °C until the dye front had completely run off the bottom of the gels. Gels were then scanned directly between the glass plates using an Ettan DIGE Imager (GE Healthcare) according to the manufacturer's instructions. Briefly, Cy2-labeled proteins, ICy3-labeled proteins and ICy5-labeled proteins were monitored with 480 nm, 540 nm and 635 nm excitation wavelengths in combination with 530 nm, 595 nm and 680 nm emission filters, respectively. Image analysis was performed using DeCyder 2-D Differential Analysis Software v7.0 (GE Healthcare) to co-detect, normalize and quantify the protein features across all of the images. Features detected from non-protein sources were filtered out. Spots displaying a ≥1.3 average-fold increase or decrease in abundance with a P value <0.05 were selected for protein identification.

2.6. Protein staining, in-gel digestion and MALDI-TOF/TOF MS analysis

Colloidal coomassie blue G-250 staining was used to visualize CyDye-labeled protein features in 2-DE followed by excised interested post-stained gel pieces for MALDI-TOF MS identification. The detailed procedures for protein staining, in-gel digestion, MALDI-TOF MS analysis and the algorithm used for data processing were described in our previous publication [18]. The spectrometer was also calibrated with a peptide calibration standard (Bruker Daltonics, Bremen, Germany) and internal calibration was performed using trypsin autolysis peaks at *m*/*z* 842.51 and *m*/*z* 2211.10. Peaks in the mass range of *m*/*z* 700–3000 were used to generate a peptide mass fingerprint that was searched against the Swiss-Prot/TrEMBL database (release on 2011_08) with 531,473 entries using Mascot software v2.3.02 (Matrix Science, London, UK). The following parameters were used: *Homo sapiens*; tryptic digest with a maximum of 1 missed cleavage; carbamidomethylation of cysteine, partial protein N-terminal acetylation, partial methionine oxidation, partial modification of glutamine to pyroglutamate, ICy3 (C34 H44 N3 O) and ICy5 (C34 H42 N3 O) and a mass tolerance of 50 ppm. Identifications were accepted based on significant MASCOT scores (P < 0.05), at least 4 peptides per protein, spectral annotation and observed *versus* expected molecular weight and p*I* on 2-DE.

2.7. Validation of thiol reactivity changes by immunoprecipitation coupled to immunoblotting

Doxorubicin treated MES-SA and MES-SA/DxR cells were lysed in the presence of ICy3 or ICy5 dyes to limit post-lysis thiol modification. The labeling reactions were performed in the dark at 37 °C for 1 h and then quenched with a 2-fold molar excess of DTT

for 10 min. 500 μg of ICy dye-labeled cell lysate was then diluted 20-fold with NP40 buffer containing protease inhibitors and then incubated with 5 μg primary antibody and 40 μL of a 50% slurry of protein A-Sepharose for 16 h at 4 °C. Immune complexes were then washed three times in lysis buffer and boiled in Laemmli sample buffer prior to resolving by SDS-PAGE. ICy images were scanned directly between low-fluorescence glass plates using an Ettan DIGE Imager (GE Healthcare) followed by immunoblotting analysis with the same primary antibody to detect the specific protein. The immunoblotting procedure is described above.

3. Results and discussion

3.1. Doxorubicin-resistance induces reduced intracellular ROS levels in MES-SA cells

Doxorubicin-induced drug resistance is one of the most serious obstacles in chemotherapy. Recent studies have indicated that reduced oxidative stress levels in cancer cells induce drug resistance. Because ROS can activate multiple signaling pathways, regulate various cellular activities and modulate disease progression, studying the molecular events related to their effects is essential. However, the redox-modifications of resistance-associated cellular targets are largely unknown. In addition, ROS are reported to modify protein cysteinyl thiol groups, leading to oxidative damage [19–21]. Hence, the current study used our previously established cysteine-labeling 2D-DIGE strategy using ICy3/ICy5 dyes to determine the altered protein thiol reactivity in a resistant uterine cancer model. The current study prepared a doxorubicin-sensitive uterine cancer cell line, MES-SA, grown in a doxorubicin-free medium containing 10% (v/v) fetal bovine serum. The MES-SA-resistant cell line, MES-SA/DxR, was grown under continuous exposure to 0.6 μM doxorubicin to maintain the multiple drug resistance phenotype, and the cells were cultured in a drug-free medium for at least 2 weeks prior to use. The IC_{50} of the MES-SA and MES-SA/DxR cells were 0.1 μM and 6 μM, respectively (Fig. 1). The MES-SA/DxR cells showed a significant up-regulation in P-glycoprotein, showing a difference in doxorubicin resistance between the 2 cell groups (data not shown). These distinctly different biochemical characteristics made these two cell lines appropriate to use as a doxorubicin-resistant cell model for a drug resistance-associated research.

Although numerous studies have observed reduced oxidative stress levels in drug resistance cancer cells, none have reported altered thiol reactivity on cysteine residues of target proteins because the free thiol group of cysteine residues is a potent nucleophilic agent that can undergo numerous redox-induced modifications under drug resistant conditions. The current study used DCF fluorescence as a readout, treating MES-SA and MES-SA/DxR cells with 0.05 μM (0.5 × IC50 of doxorubicin on MES-SA), 0.1 μM (1 × IC50 of doxorubicin on MES-SA) of doxorubicin for 20 min or left it untreated. The results indicated that MES-SA/DxR cells have a lower intracellular ROS level compared to MES-SA cells in either 0.05 μM/0.1 μM doxorubicin treatment or left without treatment (Fig. 2). Additionally, no significant redox-level alterations for MES-SA/DxR cells treated with 0 μM, 0.05 μM or 0.1 μM doxorubicin. In contrast, significant redox-level alterations for MES-SA cells treated with 0.1 μM doxorubicin in comparison with MES-SA cells treated with 0 μM or 0.05 μM doxorubicin (Fig. 2). These observations imply that resistant cells maintain higher concentrations of intracellular reduced thiol groups than drug sensitive cells. During doxorubicin treatment, high concentrations of intracellular reduced thiol groups on proteins or on small biomolecules such as glutathione are able to protect resistant cells from doxorubicin-induced ROS damage.

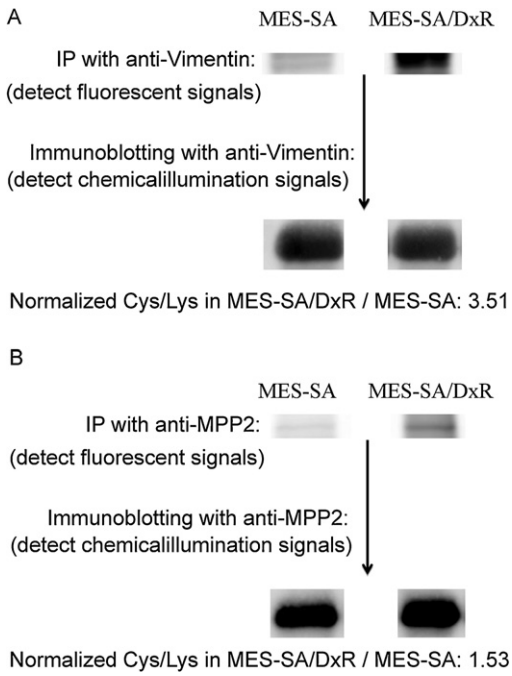

Fig. 5. Validation of the thiol reactive proteins, (A) vimentin and (B) MPP2, identified through redox-proteomic study in MES-SA and MES-SA/DxR cells by IP-WB. ICy dye-labeled protein samples from MES-SA and MES-SA/DxR cells were immunoprecipitatied with vimentin and MPP2 antibody to confirm the alterations of thiol reactivity in vimentin and MPP2, respectively, with Ettan DIGE imager (top panels). Immunoblotting against the corresponding antibody was performed to gain the protein level (bottom panels). The normalized ratios between ICy dye signal and protein immunoblotted level were shown in the figure. The standardized abundances between ICy dye signal and NHS-Cy2 signal from DeCyder software were shown in Table 1.

3.2. Redox proteomic analysis of doxorubicin-induced cysteine modifications of MES-SA and MES-SA/DxR proteins

Drug resistance has been reported to increase the intracellular antioxidant levels that remove excess ROS generated by doxorubicin treatment (see Section 1). Thus, the current study tested whether doxorubicin resistance-induced intracellular redox-alteration might modulate cellular protein function by modifying their cysteinyl thiol groups. Hence, the current study applied a recently developed redox 2D-DIGE strategy using iodoacetylated ICy dyes [22] to assess doxorubicin resistance-induced changes in MES-SA protein thiol reactivity. MES-SA and MES-SA/DxR cells were lysed in the presence of triplicate ICy5. Individual ICy5-labeled samples were then run on 2D gels against an equal load of an ICy3-labeled standard pool comprising an equal mixture of both sample types to aid in spot matching and to improve quantification accuracy (Fig. 3). The ICy5-labeled samples were subsequently labeled with lysine labeling Cy2 dye as an internal protein level control, which was used to normalize the corresponding ICy5/ICy3 signals. Significant statistical analysis and CCB post-staining enable confident identification of 33 spots by MALDI-TOF peptide mass fingerprinting analysis (Table 1 and Fig. 4). For example, redox-2D-DIGE combining the peptide mass fingerprinting profile listed in Fig. 4A contributes to identifying 54 kDa vimentin, showing a 1.70-fold increase in ICy signals in MES-SA/DxR cells rather than in MES-SA cells. Subsequent validation of the altered thiol reactivity of the identified proteins by combined immunoprecipitation with immunoblotting showed that the free thiol group levels increased for 3.51-fold in MES-SA/DxR cells rather than that in MES-SA cells (Fig. 5A). The results further confirm the accuracy of redox-2D-DIGE on monitoring the changes of free thiol content of drug

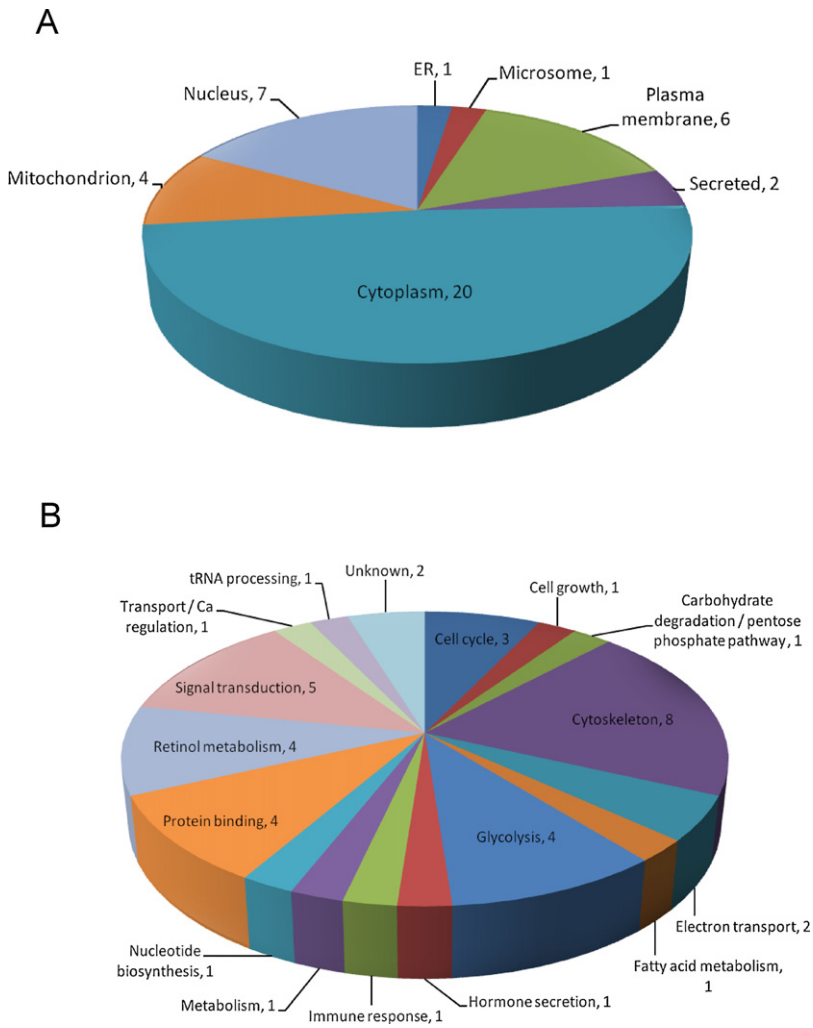

Fig. 6. Distribution of differential ICy-labeled proteins between MES-SA and MES-SA/DxR cells according to (A) subcellular location and (B) biological function.

resistant modulated proteins. The same experimental design also confirmed that MPP2 increased free thiol contents in resistant MES-SA (Fig. 5B). The differentially labeled proteins were mostly cytoplasmic and fell into several functional groups including the cytoskeleton, signal transduction, redox-regulation, glycolysis and cell cycle regulation (Fig. 6).

The ICy labeling data supports the hypothesis that doxorubicin-induced resistance induces free thiol formation in certain proteins by disrupting disulfide bonds. In addition, doxorubicin-induced resistance generated ROS might directly oxidize thiol groups to form the sulfenic, sulfinic or sulfonic acid forms of cysteine, which do not interact with ICy dyes. These thiol modifications have been reported to perturb the normal protein functions [23]. The current study examined the molecular mechanisms of doxorubicin-induced resistance in uterine cancer cells *in vitro*. Using redox-2D-DIGE and MALDI-TOF MS, the current study identified 33 doxorubicin resistance-modulated alterations in protein thiol reactivity between MES-SA and MES-SA/DxR cells. The results indicate that this approach identifies broad-ranging signatures in response to doxorubicin-induced multi-drug resistance, with the altered protein thiol reactivity having main roles in the cytoskeleton, signal transduction, redox-regulation, glycolysis and cell cycle regulation. For example, the alpha-enolase, triphosphate isomerase and pyruvate kinase isozymes M1/M2 are both glycolytic enzymes that showed an increase in ICy dye labeling in the resistance line (Table 1). Their cysteine residues reduce and generate new thiol groups for ICy labeling, implying possible redox-modulation and deregulation of these proteins. These observations suggest that modulating glycolysis enzymes redirects carbohydrate fluxes into the pentose phosphate pathway to generate increased reducing power in NADPH at the expense of glycolysis, to form a more reduced intracellular environment for drug resistance. In contrast, redox-regulation proteins, such as aldehyde dehydrogenase and peroxiredoxin 1/2 found to be decreased ICy dye-labeling in MES-SA/DxR (Table 1). Their free thiol groups must be oxidized in the resistance line to block ICy labeling, implying possible oxidative damage and deregulation of these proteins. Notably, 25 of the 33 thiol reactivity-altered spots increased ICy dye labeling in MES-SA/DxR, implying that free thiol group formation occurs in most of the identified thiol reactivity-altered proteins. This observation agrees with the current DCF assay result, which shows the reduced oxidative stress levels in resistant cancer cells.

In the current redox-proteomic analysis of differential proteomes between MES-SA and MES-SA/DxR, the current study identified the mPR protein that significantly reduced ICy dye labeling, suggesting that the mPR free thiol groups must be oxidized in the resistance line to block ICy labeling and the oxidation of the reduced cysteines on mPR might account for the development of doxorubicin-induced drug resistance. The mPR protein is involved in controlling cancer cell proliferation and growth through direct interaction between its cytochrome b5-binding domain and target proteins, combined with induced Akt phosphorylation to promote

cell survival [24–26]. Numerous cancer cells also overexpress mPR compared to normal cells, and thus, mPR is an important disease marker for cancer detection and cancer progression [27,28]. Accordingly, further study might evaluate whether the oxidation of reduced mPR contributes to the modulation of cell proliferation and growth as well as tumirogenesis.

Although cysteine labeling based 2D-DIGE can be used to monitor altered thiol reactivity of target proteins, this technique includes certain limitations in this study. First, the cysteine-labeling 2D-DIGE experiment is based on fluorescence-based protein thiol group quantification, which can detect the picogram level of ICy dye-labeled proteins; in contrast, the current post-staining experiment is based on modified CCB staining with sensitivity to 20 ng [17]. The fluorescent scanner can detect numerous differentially ICy dye-labeled low-abundant proteins that CCB staining fails to visualize. This is why more than 30% of differentially labeled features on cysteine-labeling 2D-DIGE can be chosen for MALDI-TOF MS identification. Secondly, the cysteine labeling 2D-DIGE technique can only be used to monitor the free thiol group modifications on cysteine residues; however, this technique cannot determine what types of cysteine modifications (sulfenic, sulfinic, sulfonic or glutathionated modifications) occur. Finally, the cysteine labeling strategy uses a high dye-to-protein ratio (80 pmol dye/μg protein) for redox-2D-DIGE analysis to increase detection sensitivity of thiol containing proteins. However, the high dye-to-protein level increases protein precipitation and reduces the total resolved protein spots.

4. Conclusion

The current study offers insight into doxorubicin-induced resistance mechanisms in uterine cancer and shows a link between ROS generation/removal and the cell resistance process. The current findings may have clinical implications because doxorubicin treatment has been routinely used in destroying fast growing cancer cells in a high percentage of drug resistance cases. The identified targets may also be useful for further evaluating their roles in drug-resistance formation.

Acknowledgements

This work was supported by NSC grant (100-2311-B-007-005 and 101-2311-B-007-011) from National Science Council, Taiwan, NTHU and Toward Word-Class University project from National Tsing Hua University (100N2051E1).

References

[1] H. Lage, An overview of cancer multidrug resistance: a still unsolved problem, Cell Mol. Life Sci. 65 (2008) 3145–3167.
[2] S. Verma, S. Dent, B.J. Chow, D. Rayson, T. Safra, Metastatic breast cancer: the role of pegylated liposomal doxorubicin after conventional anthracyclines, Cancer Treat. Rev. 34 (2008) 391–406.
[3] R. Vatsyayan, P. Chaudhary, P.C. Lelsani, P. Singhal, Y.C. Awasthi, S. Awasthi, S.S. Singhal, Role of RLIP76 in doxorubicin resistance in lung cancer, Int. J. Oncol. 34 (2009) 1505–1511 (review).
[4] A.E. Green, P.G. Rose, Pegylated liposomal doxorubicin in ovarian cancer, Int. J. Nanomedicine 1 (2006) 229–239.
[5] S.T. Lin, H.C. Chou, S.J. Chang, Y.W. Chen, P.C. Lyu, W.C. Wang, M.D. Chang, H.L. Chan, Proteomic analysis of proteins responsible for the development of doxorubicin resistance in human uterine cancer cells, J. Proteomics 75 (2012) 5822–5847.
[6] E. Rollet-Labelle, M.J. Grange, C. Elbim, C. Marquetty, M.A. Gougerot-Pocidalo, C. Pasquier, Hydroxyl radical as a potential intracellular mediator of polymorphonuclear neutrophil apoptosis, Free Radic. Biol. Med. 24 (1998) 563–572.
[7] H. Tanaka, I. Matsumura, S. Ezoe, Y. Satoh, T. Sakamaki, C. Albanese, T. Machii, R.G. Pestell, Y. Kanakura, E2F1 and c-Myc potentiate apoptosis through inhibition of NF-kappaB activity that facilitates MnSOD-mediated ROS elimination, Mol. Cell 9 (2002) 1017–1029.
[8] D.G. Smith, T. Magwere, S.A. Burchill, Oxidative stress and therapeutic opportunities: focus on the Ewing's sarcoma family of tumors, Expert Rev. Anticancer Ther. 11 (2011) 229–249.
[9] K.D. Tew, M. O'Brien, N.M. Laing, H. Shen, Coordinate changes in expression of protective genes in drug-resistant cells, Chem. Biol. Interact. 111/112 (1998) 199–211.
[10] R.P. Perez, T.C. Hamilton, R.F. Ozols, R.C. Young, Mechanisms and modulation of resistance to chemotherapy in ovarian cancer, Cancer 71 (1993) 1571–1580.
[11] G.C. Das, A. Bacsi, M. Shrivastav, T.K. Hazra, I. Boldogh, Enhanced gamma-glutamylcysteine synthetase activity decreases drug-induced oxidative stress levels and cytotoxicity, Mol. Carcinog. 45 (2006) 635–647.
[12] K. Kahlos, Y. Soini, R. Sormunen, R. Kaarteenaho-Wiik, P. Paakko, K. Linnainmaa, V.L. Kinnula, Expression and prognostic significance of catalase in malignant mesothelioma, Cancer 91 (2001) 1349–1357.
[13] L.I. McLellan, C.R. Wolf, Glutathione and glutathione-dependent enzymes in cancer drug resistance, Drug Resist. Updat. 2 (1999) 153–164.
[14] J.F. Timms, R. Cramer, Difference gel electrophoresis, Proteomics 8 (2008) 4886–4897.
[15] H.C. Chou, Y.C. Lu, C.S. Cheng, Y.W. Chen, P.C. Lyu, C.W. Lin, J.F. Timms, H.L. Chan, Proteomic and redox-proteomic analysis of berberine-induced cytotoxicity in breast cancer cells, J. Proteomics 75 (2012) 3158–3176.
[16] C.L. Wu, H.C. Chou, C.S. Cheng, J.M. Li, S.T. Lin, Y.W. Chen, H.L. Chan, Proteomic analysis of UVB-induced protein expression- and redox-dependent changes in skin fibroblasts using lysine- and cysteine-labeling two-dimensional difference gel electrophoresis, J. Proteomics 75 (2012) 1991–2014.
[17] H.L. Chan, S. Gharbi, P.R. Gaffney, R. Cramer, M.D. Waterfield, J.F. Timms, Proteomic analysis of redox- and ErbB2-dependent changes in mammary luminal epithelial cells using cysteine- and lysine-labelling two-dimensional difference gel electrophoresis, Proteomics 5 (2005) 2908–2926.
[18] T.C. Lai, H.C. Chou, Y.W. Chen, T.R. Lee, H.T. Chan, H.H. Shen, W.T. Lee, S.T. Lin, Y.C. Lu, C.L. Wu, H.L. Chan, Secretomic and proteomic analysis of potential breast cancer markers by two-dimensional differential gel electrophoresis, J. Proteome. Res. 9 (2010) 1302–1322.
[19] M. Kemp, Y.M. Go, D.P. Jones, Nonequilibrium thermodynamics of thiol/disulfide redox systems: a perspective on redox systems biology, Free Radic. Biol. Med. 44 (2008) 921–937.
[20] J.V. Cross, D.J. Templeton, Regulation of signal transduction through protein cysteine oxidation, Antioxid. Redox. Signal. 8 (2006) 1819–1827.
[21] L.K. Moran, J.M. Gutteridge, G.J. Quinlan, Thiols in cellular redox signalling and control, Curr. Med. Chem. 8 (2001) 763–772.
[22] H.L. Chan, P.R. Gaffney, M.D. Waterfield, H. Anderle, M.H. Peter, H.P. Schwarz, P.L. Turecek, J.F. Timms, Proteomic analysis of UVC irradiation-induced damage of plasma proteins: Serum amyloid P component as a major target of photolysis, FEBS Lett. 580 (2006) 3229–3236.
[23] P. Ghezzi, V. Bonetto, M. Fratelli, Thiol-disulfide balance: from the concept of oxidative stress to that of redox regulation, Antioxid. Redox. Signal. 7 (2005) 964–972.
[24] H. Neubauer, G. Adam, H. Seeger, A.O. Mueck, E. Solomayer, D. Wallwiener, M.A. Cahill, T. Fehm, Membrane-initiated effects of progesterone on proliferation and activation of VEGF in breast cancer cells, Climacteric 12 (2009) 230–239.
[25] T. Yang, P.J. Espenshade, M.E. Wright, D. Yabe, Y. Gong, R. Aebersold, J.L. Goldstein, M.S. Brown, Crucial step in cholesterol homeostasis: sterols promote binding of SCAP to INSIG-1, a membrane protein that facilitates retention of SREBPs in ER, Cell 110 (2002) 489–500.
[26] H. Neubauer, S.E. Clare, W. Wozny, G.P. Schwall, S. Poznanovic, W. Stegmann, U. Vogel, K. Sotlar, D. Wallwiener, R. Kurek, T. Fehm, M.A. Cahill, Breast cancer proteomics reveals correlation between estrogen receptor status and differential phosphorylation of PGRMC1, Breast Cancer Res. 10 (2008) R85.
[27] J. Xu, C. Zeng, W. Chu, F. Pan, J.M. Rothfuss, F. Zhang, Z. Tu, D. Zhou, D. Zeng, S. Vangveravong, F. Johnston, D. Spitzer, K.C. Chang, R.S. Hotchkiss, W.G. Hawkins, K.T. Wheeler, R.H. Mach, Identification of the PGRMC1 protein complex as the putative sigma-2 receptor binding site, Nat. Commun. 2 (2011) 380.
[28] M.A. Cahill, Progesterone receptor membrane component 1: an integrative review, J. Steroid Biochem. Mol. Biol. 105 (2007) 16–36.